

Internal Mode Structure of Resonant Field Amplification in DIII-D

M.J. Lanctot¹, I.N. Bogatu², A.M. Garofalo³, Y. In², G.L. Jackson³, R.J. La Haye³,
G. A. Navratil¹, M. Okabayashi⁴, H. Reimerdes¹, W.M. Solomon⁴, E.J. Strait³,
and A.D. Turnbull³

¹ Columbia University, New York, New York 10027, USA

²FAR-TECH, Inc., San Diego, USA

³General Atomics, PO Box 85608, San Diego, California 92186-5608, USA

⁴Princeton Plasma Physics Laboratory, PO Box 451, Princeton, New Jersey, 08543-0451 USA

I. Introduction

Sustained operation at high- β_N [$= \beta/(I/aB)$] in tokamak plasmas requires the minimization of magnetic field asymmetries ($10^{-4} B_o$) known as “error fields.” The sensitivity of high- β plasmas to error fields is caused by a plasma response to fields that are resonant with weakly-damped resistive wall modes (RWM), a phenomenon referred to as resonant field amplification (RFA) [1]. In the vacuum between the plasma and the vessel wall at the outer midplane, the perturbed field due to the RFA is well described by a single mode model put forth by Garofalo, Jensen, and Strait [2]. The success of the model motivated the development of “active MHD spectroscopy”, which uses slowly rotating magnetic perturbations to drive the RFA, and magnetic sensor arrays to monitor the macroscopic stability [3]. The good agreement between the observed and predicted spectral response of the RFA suggests that the internal RFA mode structure should be consistent with the structure of the ideal MHD external kink mode. Here we compare the observed internal structure of the RFA in DIII-D using soft x-ray cameras (SXR) to results from a virtual SXR diagnostic based on ideal MHD calculations of the $n = 1$ external kink structure using GATO [4].

II. Internal Mode Structure Measurements

A pair of 12-channel SXR diode cameras, separated toroidally by 120° , are used to observe the 3-dimensional internal structure of non-axisymmetric perturbations of the plasma. A $127 \mu\text{m}$ beryllium foil is used to filter out line emission from plasma impurities. Thus, a good approximation to the observed SXR emission is given by the spectrally integrated formula for electron brehmsstrahlung and recombination radiation in a Maxwellian plasma. In this case, the i^{th} diode signal is proportional to the line integral over the plasma region L_i observed by the diode active area [5],

$$S_{o,i}(t) \propto \int_{L_i} Z_{eff}(\psi,t) n_e^2(\psi,t) T_e^{1/2}(\psi,t) e^{-\frac{E_{cut}}{T_e(\psi,t)}} dL_i \quad ,$$

where ψ is the poloidal flux, Z_{eff} is the plasma effective charge, n_e and T_e are the electron density and temperature, and E_{cut} (≈ 2 keV) is the Be filter cutoff energy.

The RFA measurements were made in single null diverted H-mode plasmas with $q_{95} = 4.7$. Following the L-H transition, 10 MW of neutral beam power is used to reach a β_N of 2.4, Fig. 1(a). DCON [6] calculations show that this value of β_N is above the $n = 1$ no-wall limit of $\beta_N = 2.0$. The no-wall limit in these discharges scales with 2.4 times the internal inductance. However, these discharges are below the ideal wall limit of $\beta_N = 3.0$, so that the $n = 1$ kink mode is stabilized by the resistive vacuum vessel wall and the toroidal plasma rotation, which is driven by neutral beam injection [7]. The RFA is driven to a finite amplitude by a set of 12 coils (I-coil) located between the plasma facing graphite tiles and the vacuum vessel [8]. The individual coils are connected so the applied $n = 1$ field matches the expected helicity of the RWM. The I-coil currents are modulated so the field rotates near the natural rotation frequency of the mode, which is 10-20 Hz in the direction of the toroidal plasma rotation [3].

An in-vessel spatial alignment of the SXR cameras assures that two viewing chords from toroidally separated cameras view an equivalent region of the plasma. The difference of these signals, ΔS_i , is non-zero in the presence of any non-axisymmetric perturbation, but is unaffected by axisymmetric changes to the emissivity. We assume that the ΔS_i are due solely to the $n = 1$ mode. This assumption is justified by the absence of higher n perturbations in the signals from the midplane Mirnov probe array at the frequency of the applied I-coil field. The RFA can be observed clearly in the ΔS_i signals, Fig. 1(c). The amplitude and phase of the perturbation for each chord pair is determined using Fourier analysis, or a least squares fitting routine. Note that the SXR measurements are made during a time period when the driven mode is stable, and β_N and the amplitudes of the ΔS_i are nearly constant.

III. Comparison with GATO

To compare the SXR measurements with ideal MHD calculations, we used a synthetic or virtual diagnostic approach (VDA). Given the geometry of the SXR viewing chords [Fig. 2(a)],

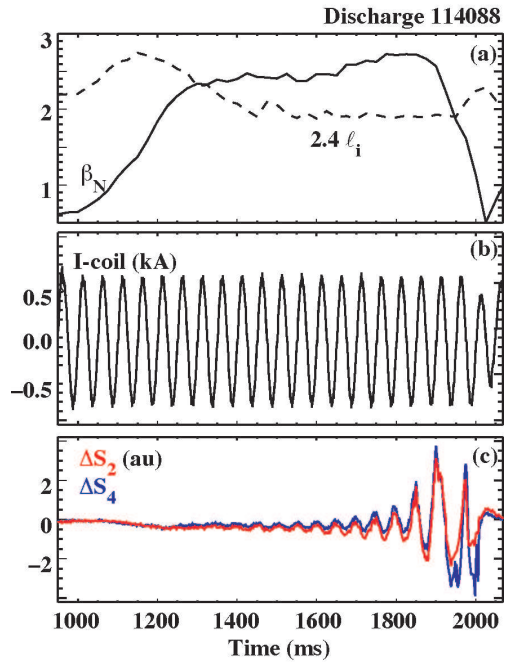


Figure 1: (a) With β_N above the no-wall limit, (b) the I-coil applies a rotating field at 20 Hz. (c) The RFA is observed on the ΔS_i .

the VDA is more appropriate because the inverse problem is ill-posed. In the VDA, an equilibrium reconstruction, constrained by internal current and kinetic profile measurements using the EFIT code [9], is used as input to GATO, which calculates the growth rate and mode displacement, ξ , of the unstable free boundary $n = 1$ kink mode. The GATO calculation was done without a wall at the location of the DIII-D vessel. The effect of a wall on the mode structure will be examined in a future study. The relevant component of ξ is in the $\nabla\psi$ direction since a displacement in this direction will either increase or decrease the magnitude of the observed signal. We write the total signal, S_i , as the sum of an equilibrium component $S_{o,i}$ and a perturbation ΔS_i^m . A quantity for ΔS_i^m is determined using the profiles for n_e and T_e from Thomson scattering and an electron cyclotron emission radiometer, with the assumptions that the Z_{eff} is constant across the profile, and the SXR profile is convected with the mode displacement.

$$S_i = S_{o,i} + \Delta S_i^m = S_{o,i} + \int_{L_i} \xi \cdot \nabla\psi \frac{\partial s_o}{\partial \psi} \sin\theta dL_i \quad ,$$

where ΔS_i^m is the simulated perturbation, s_o is the equilibrium emissivity, and θ is the angle between the line of sight and the $\nabla\psi$ direction. Since the RFA structure is rotating, it is necessary to compute the line integrals at two toroidal locations to resolve the $n = 1$ amplitude and relative phase of ΔS_i^m to compare with the analysis of the ΔS_i signals. ΔS_i^m was calculated using the profiles from discharge 114084 and a GATO calculation for the same discharge, shown in Fig. 2(b) as a function of toroidal angle.

IV. Discussion and Summary

Using channel 3 as a reference to normalize the amplitude and phase of the VDA prediction to measurements from 114084, we find good agreement for channels 1-7 (Fig. 3). The phase shift near chord 5 is observed in the measurements and modeled signals, see Fig. 2(b). The good agreement observed in the core supports previous experimental results that identified the RFA as the driven RWM stabilized by toroidal plasma rotation. However, with this normalization, outside of the $q = 2$ surface, the modeled amplitudes overestimate the perturbed signal. The large edge perturbation predicted by the VDA is caused by peaks in the displacement near

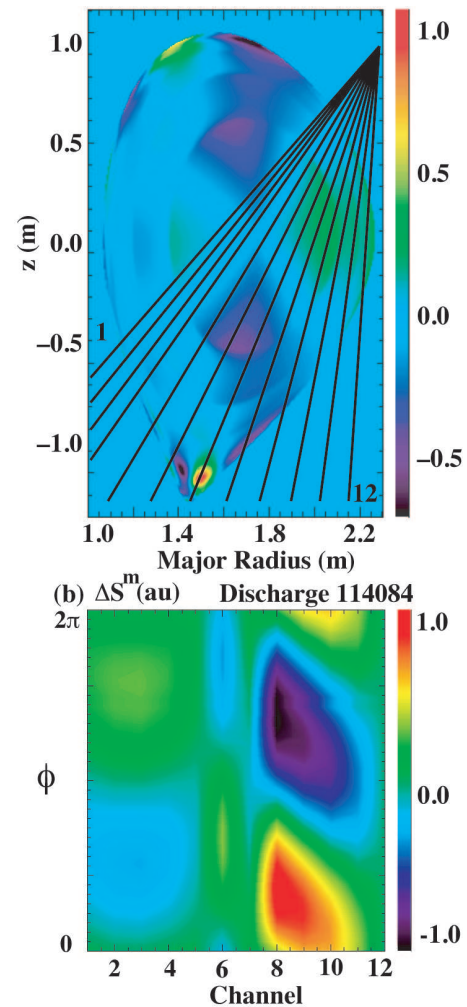


Figure 2: (a) Normalized $\xi \cdot \nabla\psi$ from GATO with centerlines of SXR viewing chords. (b) Modeled ΔS^m as a function of toroidal angle.

the rational q surfaces predicted by GATO for a free-boundary equilibrium above the no-wall limit.

The failure of the virtual diagnostic to recreate all of the measurements calls into question the accuracy of the SXR data analysis method and the stability modeling. Previous reports of T_e and B_z perturbations due to the RFA do show a peak near the $q = 2$ surface [10] so the absence of this peak in the SXR data means that either the previously observed peak is due to the $n = 0$ perturbation, or that errors in the SXR spatial calibration resulted in a reduction of the calculated $n = 1$ amplitude. Efforts to improve the measurement will utilize a third SXR camera to reduce errors in measuring the $n = 1$ component of the mode. In terms of the

modeling, a number of issues are currently being investigated. First, the calculated mode structure for a free boundary equilibrium may be different depending on which stability code is used. For example, GATO includes inertia effects while the DCON code neglects inertia when minimizing the potential energy. The mode structure may also be modified by the presence of a resistive wall near the plasma surface, or by plasma rotation. These effects are being modeled in the MARS stability code. A comparison of the mode structure from all three codes with measurements of the RFA will help to further characterize RFA and test RWM stability models.

This work was supported by the US Department of Energy under DE-FG02-89ER54461, DE-FG02-03ER83657, DE-FC02-04ER54698, and DE-AC02-76CH03073.

References

- [1] A.H. Boozer, *Phys. Rev. Lett.* **86**, 5059 (2001)
- [2] A.M. Garofalo, T.H. Jensen, and E.J. Strait, *Phys. Plasmas* **10**, 4776 (2003)
- [3] H. Reimerdes et al., *Phys. Rev. Lett.* **93**, 135002 (2004)
- [4] L.C. Bernard, F.J. Helton, and R.W. Moore, *Comput. Phys Commun.* **21**, 377 (1981)
- [5] I.H. Hutchinson, (1983), *Princ. of Plasma Diagnostics*, Cambridge Univ. Press
- [6] A.H. Glasser and M.S. Chance, *Bull. Am. Phys. Soc.* **42**, 1848 (1997)
- [7] E.J. Strait et al., *Phys. Rev. Lett.* **74**, 2483 (1995)
- [8] G.L. Jackson, et al., Proc. 30th EPS Conf. on Controlled Fusion and Plasma Physics, St. Petersburg, Russia, 2003, European Physical Society, Vol. 27A
- [9] L.L. Lao et al., *Fusion Sci. Technol.* **48**, 968, (2005)
- [10] R.J. Jayakumar et al., *Rev. Sci. Instrum.*, **75**, 2995, (2004)

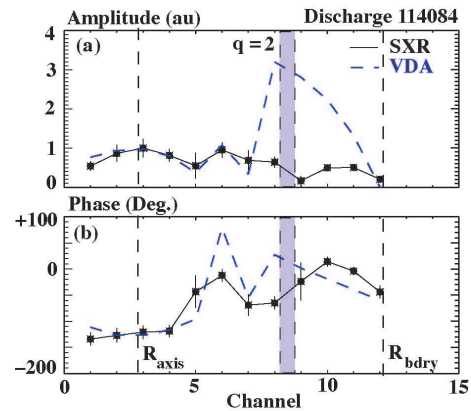


Figure 3: Comparison of (a) amplitude and (b) phase of ΔS_i^m with SXR data from 114084.